

Gravity anomalies, flexure, and deformation of the converging Indian lithosphere in Nepal and Sikkim–Darjeeling Himalayas

Md. Afroz Ansari · Prosanta K. Khan ·
Virendra M. Tiwari · Jayashree Banerjee

Received: 6 October 2013 / Accepted: 27 May 2014 / Published online: 17 June 2014
© Springer-Verlag Berlin Heidelberg 2014

Abstract Researchers ubiquitously noted that the common processes of partitioning oblique convergence in response to drag from the trench-hanging plate simultaneously produce radial slips, along-strike translation, and extension parallel to the deformation front. Here, we focus on the area between Nepal and Sikkim–Darjeeling Himalayas, and carry out gravity and finite-element stress modeling of the strike-orthogonal converging Indian lithosphere. We delineate the geometries of different layers and their interfaces through gravity modeling. The optimum model parameters along with rheological parameters of different layers are used for finite-element modeling. Finite-element modeling is done with boundary conditions of keeping the upper surface free and rigidly fixing the section of the northern boundary below the Main Himalayan Thrust. We impart on its frontal section an amount of 6×10^{12} N/m force, equivalent to resistive force of the Himalayan–Tibet system, and analyze the maximum and minimum compressive stress fields evolved in the lithosphere. We testify our observations with earthquake database and other geophysical and geological studies. We note that an increasing flexing of the Indian lithosphere beyond the Main Boundary Thrust becomes maxima between the Main Central Thrust and South Tibetan Detachment in both the areas; however, more steepening of the Moho boundary is identified in the Sikkim–Darjeeling Himalaya. This abrupt change in lithospheric geometry beneath the Greater Himalaya is likely correlated with the sharp elevation changes in the

topography. Although the highest seismicity concentration is dominant in this zone, the Lesser and the Tethys Himalayas in Sikkim–Darjeeling area also record relatively fair seismic activity. More compressive stress field in different layers right within the sharp bending zone supports this observation. We thus propose that the sharp bending zone beneath the Greater Himalaya is suffering maximum deformation, and the deformation is continued in the mantle too. We also identify both right-lateral shear and radial vergence slip, which are presumably associated with the general dynamics and kinematics of the Himalaya.

Keywords Flexing · Deformation · Stress field · Seismicity · Plate obliquity

Introduction

The Himalayan range is a diffused plate boundary evolved through continental collision between the Indian land mass and the Asia, and began at some 50 Ma before (Besse et al. 1984; Molnar 1984; Patriat and Achache 1984; Gaetani and Garzanti 1991). The convergence rates of Indian plate against the southern margin of the Tibetan plateau vary significantly between ~4.2 and 5.4 cm/years (DeMets et al. 1990). The convergence led to the tectonic stacking of upper and mid-crustal slabs on the northern margin along the foreland of the Indian plate originating from the basal decollement called the Main Himalayan Thrust (MHT). The compression due to convergence and stacking of crustal slabs over the leading edge of the Indian plate results its flexure and progressive thickening of the crust toward the north (Lyon-Caen and Molnar 1985). The weight of the mountains is supported in part by the strength of the plate, and the plate distributes the load by flexing down in front

M. A. Ansari · P. K. Khan (✉) · J. Banerjee
Department of Applied Geophysics, Indian School of Mines,
Dhanbad, India
e-mail: pkkhan_india@yahoo.com

V. M. Tiwari
National Geophysical Research Institute, Hyderabad, India

of the range to form a basin (e.g., Lyon-Caen and Molnar 1983). The Moho configuration of the lithosphere beneath the Greater Himalaya toward north accounts for decrease in flexural rigidity (Jin et al. 1996; Cattin et al. 2001; Jordan and Watts 2005; Hetényi et al. 2006; Tiwari et al. 2006, 2010). Gravity data show an increase in gravity gradient from ~ 1 mgal km^{-1} over the Indo-Gangetic plain to 2 mgal km^{-1} over the Greater Himalaya, which accounts for more steepening of the Moho beneath the Greater Himalaya (i.e., $\sim 10^\circ$ – 15°) than beneath the Lesser Himalaya (i.e., $\sim 2^\circ$ – 3°) (Molnar 1983; Ni and Barazangi 1984). The seismic experiments conducted in southern Tibet indicate a crustal thickness of the order of 70–80 km (e.g., Hirn et al. 1984; Zhao et al. 1993; Nelson et al. 1996), consistent with isostatic adjustment of the plateau (Lyon-Caen and Molnar 1985; Jin et al. 1996; Hetényi et al. 2006; Tiwari et al. 2006, 2010). Tectonic crustal thickening associated with deformation in the Himalaya is in part compensated by denudation (Cattin and Avouac 2000); however, the denudation rates vary laterally along the stretch of the Himalayan arc (Cattin and Avouac 2000). Lavé and Avouac (2000) have shown that the localized thrust faulting on the Main Frontal Thrust (MFT) is continued along the MHT and absorbs ~ 22 mm/years, an amount that accounts for all shortening rate across the range. This is in agreement for thrusting of the Himalaya over the MHT with little internal deformation (Cattin and Avouac 2000). Li et al. (2008) advocated a significant lateral variations in subduction-related mantle structure beneath the Himalayan collision zone and inferred that the horizontal distance over which the Indian lithosphere slides northward beneath the plateau decreases from west to east.

Our study area is focused over two important tectonic domains of the Himalayas: (1) the Nepal and (2) the Sikkim–Darjeeling sector (Fig. 1a). Along with north-south variations of tectonic processes all through the ~ 2500 km long Himalayan belt (Ni and Barazangi 1984; Hodges 2000), there is significant west-east variations of topography (Duncan et al. 2003; Yin 2006; Khan et al. 2014), a reduction in crustal shortening (McQuarrie et al. 2008; Long et al. 2011), decrease in flexural wavelength (Hammer et al. 2013) and patterns of focal mechanisms (Hazarika et al. 2010). Besides, the Indian plate obliquity increases both toward west and east of Kathmandu, Nepal, and reaches to highest values at the termini of the Himalayan orogen (McCaffery 1996). Northward penetrating evenly spaced basement ridges (e.g., Monghyr-Saharsa, Faizabad, and Delhi–Hardwar) in the central sector of the Himalayan foothill (Sastri et al. 1971; Rao 1973; Valdiya 1976; Dasgupta et al. 1987; Gahalaut and Kundu 2012), uneven along-strike distribution of seismicity (Ni and Barazangi 1984; Khattri 1987; Verma and Kumar 1987; Bilham and Gaur 2000; Rajendran and Rajendran 2005), counterclockwise rotational underthrusting, oroclinal

bending and the consequent southward non-uniform migration of overriding land mass toward the Himalayan margin (Klootwijk et al. 1985; Willet and Beaumont 1994), and the confinement of earthquakes in the deeper part of the converging Indian lithosphere (Nábelek et al. 2009; Ansari and Khan 2013) clearly envisage a lateral change in dynamics/kinematics of the Himalaya. In line with these evidences, we examine the gravity data through modelling of Nepal and Sikkim–Darjeeling sectors of this intercontinental diffuse boundary. We note an apparent change in dip of the Moho between these regions. We further testify our observations through finite-element stress modelling and earthquake's source processes in these areas. Two trench-orthogonal vertical models for the oppositely converging Indian lithosphere and the Asian land mass for Nepal as well as Sikkim–Darjeeling Himalayas have been proposed through improving model parameters for geometry and density of each prism by linear inversion (Webring 1985). To minimize the non-uniqueness of the modeling, the initial geometries of different layers and crustal boundaries within the converging Indian lithosphere and the overriding Asian land mass (Fig. 1b) have been initially constrained by the works of Owens and Zandt (1997), Johnson (2002), Thiede et al. (2004), Bollinger et al. (2006), Robert et al. (2009), Zhang and Klemperer (2010), and Hammer et al. (2013).

During the last two decades, numerical modeling has been widely used to explore the stress field and mechanics of lithospheric deformation in different tectonic regimes of the world (Makel and Walters 1993; Willett et al. 1993; Beaumont et al. 1994; Sassi and Faure 1997; Vanbrabant et al. 1999; Mikhailov and Marin 2001) and also in the Himalayan arcuate belt (Wang and Shi 1982; Singh et al. 1990; Vergne et al. 2001; Sanker et al. 2002; Berger et al. 2004). We also do the finite-element modeling on the converging lithosphere, delineated through gravity modeling, for understanding the local deformation in the crust and mantle, and also along crustal discontinuities. We further analyze 114 earthquake events (magnitude ≥ 4.0) occurring during the period 1902 to 2012 in these sectors of the Himalayan arcuate belt (Fig. 2). The earthquake data were taken from the catalogues of Indian Society of Earthquake Technology (Bapat et al. 1983), International Seismological Centre, and US Geological Survey. A total of 13 focal mechanisms of earthquakes of magnitude $M_w \geq 4.7$ are also compiled from the Harvard Centroid Moment Tensor Catalogue, Chandra (1978), Molnar and Tapponnier (1978), Tandon (1972) for better understanding the deformation processes.

Tectonic framework

The Himalaya marking the southern edge of the Tibetan Plateau was built through southward transportation of

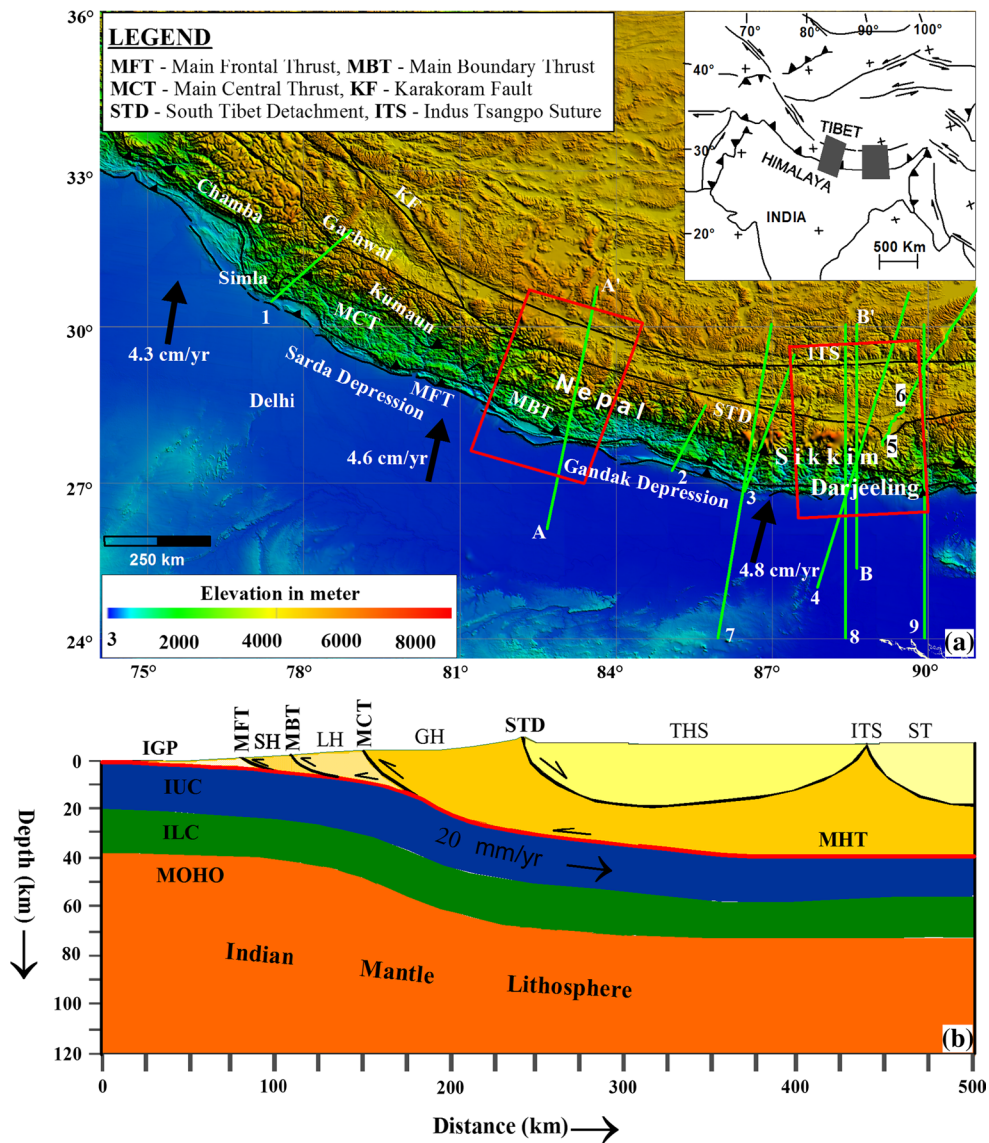


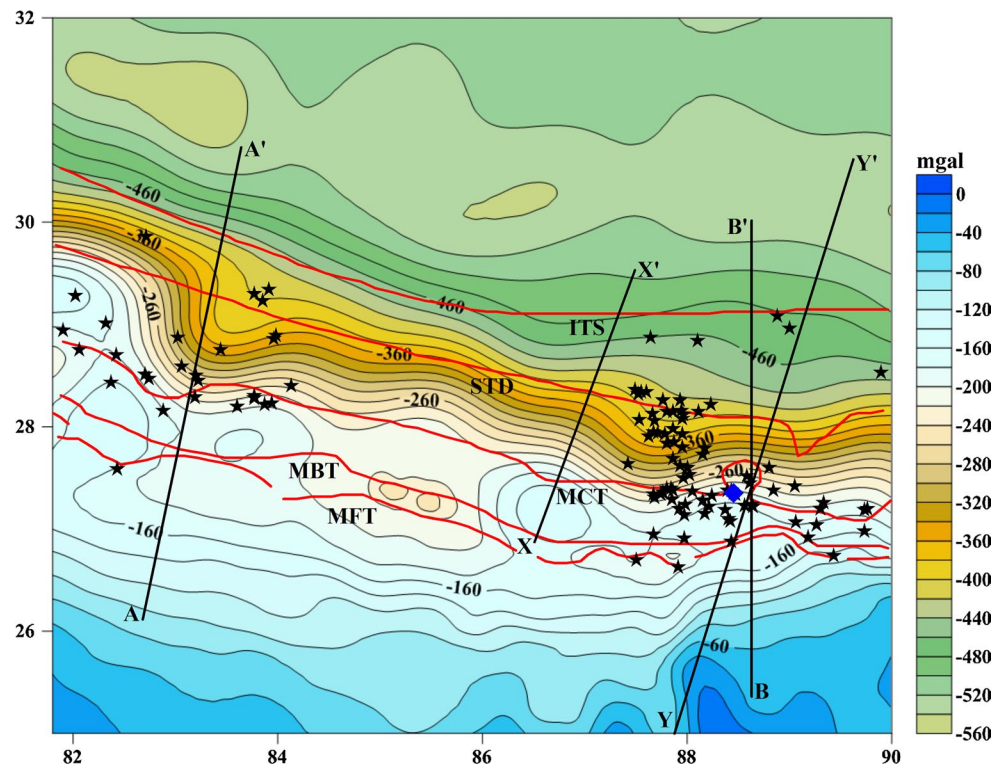
Fig. 1 **a** Simplified tectonic map with overview of topography of Nepal and Sikkim–Darjeeling Himalayas reconstructed after Gansser (1964), Valdiya (1980), Verma and Kumar (1987), Gahalaut and Kundu (2012). The shaded areas in the inset map on top right represent the study area. The topographic elevation is shown by the colored scale on left bottom corner. Solid arrows represent the convergence velocity direction of the Indian plate with respect to the Asian plate (after DeMets et al. 1994). Barbed solid triangle represents the thrusting. Various profiles (1 after Thiede et al. 2004; 2 after Bollinger et al. 2006; 3 after Schulte-Pelkum et al. 2005; 4 after Tiwari et al. 2006; 5 and 6 after INDEPTH; 7, 8, and 9 after Hammer et al. 2013) used for constraining the initial lithosphere

geometries are also shown by solid green-colored lines. Profiles AA' and BB' are considered for the present study. **b** Simplified section across the Himalaya illustrating the subduction of Indian lithosphere beneath southern Tibet (after Owens and Zandt 1997; Johnson 2002; Thiede et al. 2004; Bollinger et al. 2006; Robert et al. 2009; Zhang and Klempere 2010; Hammer et al. 2013). MFT Main Frontal Thrust, MBT Main Boundary Thrust, MCT Main Central Thrust, MHT Main Himalayan Thrust, STD South Tibetan Detachment, ITS Indus-Tsangpo Suture, SH Siwalik Himalaya, LH Lesser Himalaya, GH Greater Himalaya, THS Tethys Himalaya, ST Southern Tibet, IUC Indian Upper Crust, ILC Indian Lower Crust

thrust packages along the numbers of east–west-oriented crustal-scale discontinuities, viz., Main Central Thrust fault (MCT), Main Boundary Thrust fault (MBT), and the MFT (Le Fort 1986). Deformation of the overriding Asian land mass has been migrated southward and the MFT being the most recently activated one in the sequence (Lavé and

Avouac 2000). This fault is delineated to the top of the Indian basement at a depth of about 5 km and extends sub-horizontally beneath the Lesser Himalaya (Schelling and Arita 1991; Lavé and Avouac 2000). The MFT places the sub-Himalayan molasse belt over undeformed foreland sediments of the Indo-Gangetic plain. The basement of the

Fig. 2 Contour map illustrates the variations in Bouguer gravity anomalies across the Nepal and Sikkim–Darjeeling Himalayas reconstructed based on EGM2008 gravity model. Profiles AA' and BB' were chosen through Nepal and Sikkim–Darjeeling Himalayas for gravity modeling of the converging Indian lithosphere. A comparison of dip-angle variations in Moho boundaries is made between profiles AA' and BB' (present study) and XX' (after Schulte-Pelkum et al. 2005) and YY' (after Tiwari et al. 2006). Black stars represent the distribution of earthquake's epicenters with magnitude 4.0 and above. Note the higher concentration of seismicity in Sikkim–Darjeeling Himalayas. Solid blue rectangle represents the epicenter of 2011 Mw 6.9 Sikkim earthquake. Abbreviations are explained in the caption of Fig. 1



active Himalayan foreland basin is irregular, with several subsurface ridges extending from the Peninsula Highlands northwards to the Himalayan front. These structural highs generally trend at high angles to the Himalayan range and have structural relief locally exceeding ~2.0 km along east–west direction parallel to the Himalayan thrust front (Raiverman 2000). The sub-Himalayan belt, consisting of Miocene to Quaternary molasse exposed in the Himalayan foothills (Acharya and Ray 1977), has an average elevation of about 0.9–1.5 km (Valdiya 1988). The ruggedly youthful Siwalik domain is characterized by steep slopes, swift-flowing consequent streams, and deep valleys of antecedent rivers (Valdiya 1988). The south-vergent MBT, which appears to have been active some ~10 Ma before (Meigs et al. 1995; Burbank et al. 1996), placed the Lesser Himalayan meta-sedimentary belt over the sub-Himalayan molasse belt. The Lesser Himalayan belt consists of ~12-km-thick section of phyllites, schists, slates, and marbles (Schelling 1992). The average elevation of rising Lesser Himalaya is 1.5–2.5 km, and its sub-province shows a mild and mature topography with gentle slope toward the north (Valdiya 1988; Yin 2006). The region is characterized by several nappes of metamorphic rocks brought southward over long distances by imbricate thrusting (e.g., Le Fort 1975; Valdiya 1976, 1989; Gansser 1981). The south-vergent MCT places the Greater Himalayan crystalline belt over the Lesser Himalayan belt, resulting in upward increasing metamorphic grade within both (Hubbard and Harrison 1989).

The Main Himalayan Seismic belt is mostly confined within the MBT and MCT zones (Ni and Barazangi 1984). The Greater Himalayan belt is interpreted as a thrust sheet of Indian continental basement displaced southward along the MCT (Argand 1924; Heim and Gansser 1939; Le Fort 1975; Schelling and Arita 1991). The Great Himalaya rises to a height over 6.5–7.0 km (Valdiya 1988) over which lies the perennial snows (Yin 2006). The Greater Himalayan zone consists of 15- to 20-km-thick slab of crystalline rocks, which has been thrust southwards along the MCT, overriding the Lesser Himalayan formations (Yin 2006). Structural relations, together with the INDEPTH profiling (Hauck et al. 1998), imply that MFT, MBT, and MCT merge at depth to a single northward dipping decollement, the MHT (Schelling and Arita 1991; Zhao et al. 1993; Makovsky et al. 1996; Hauck et al. 1998; Bollinger et al. 2006). The Greater Himalayan belt is succeeded northward by the Tethyan sedimentary belt. The Tethyan belt strata were deposited on the northern passive continental margin of India (Burg and Chen 1984; Searle et al. 1987). The Greater Himalayan belt is generally considered basement of the Tethyan belt cover (Gansser 1964; Burg and Chen 1984). The Tethyan belt is succeeded northward by the Indus–Tsangpo Suture zone, which is characterized by dismembered ophiolites, radiolarian cherts, forearc flysch deposits, and tectonic mélange-containing blocks of Tethyan strata (Burg and Chen 1984). The composite Gangdese batholiths of Cretaceous to Eocene age (Schärer et al. 1984;

Debon et al. 1986; Copeland et al. 1995) lies immediately north of the suture.

Gravity modeling

Several new global gravity models (EIGENGL04C, Forste et al. 2008; EGM2008, Pavlis et al. 2008) are developed based on the data from GRACE/CHAMP satellite mission for long wavelengths (low degree and order of spherical harmonics) and terrestrial data for short wavelengths. Gravity field of the EIGENGL04C model is computed for spherical harmonics of degree and order 360. It combines GRACE data for spherical harmonic coefficients up to degree and order 70, amalgamation of satellite and terrestrial data at intermediate wavelength, and terrestrial data at short wavelength (higher spherical harmonics of 115–360). The EGM2008 gravity model is complete to the spherical harmonics of degree and order 2,159, and also combines primarily the satellite and surface measurements (Pavlis et al. 2008). The EGM2008 model is computed for higher spherical harmonics, and thus, its spatial resolution is relatively more than the EIGENGL04C model. The present Bouguer gravity anomaly (BGA) map (Fig. 2) is constructed from EGM2008 gravity model after incorporating Bouguer correction and all terrain corrections and compared with ground gravity data. The Bouguer anomalies are consistent with terrestrial data; however, short-wavelength anomalies are filtered for consistency. Thus, such map has potential in studying large-scale geologic features across the Himalaya, where little or no terrestrial data are available (e.g., Tiwari et al. 2010). The 2D modeling is undertaken by choosing long profile that cuts all through the main geological features of the collision zone, to understand the long-wavelength gravity anomalies. Both the profiles AA' and BB' are taken nearly orthogonal to the strike of the India–Eurasia collision zone.

One of the most common problems encountered in geophysical studies is the determination of the geometry of geological contacts at depth. Bouguer gravity anomalies reflect lateral variations in density at depth. The largest subsurface density discontinuity near the surface of earth occurs at the Moho, a chemical boundary between crust and mantle rocks. Seismic velocities also have a significant jump across the Moho. The deformation of the Moho can be used to gauge the deformation of the upper mantle of the lithosphere. The Bouguer gravity anomalies caused by heterogeneities in the distributions of masses and therefore density contrast between them can be used for delineating structures in the subsurface (Molnar 1988). Models based on gravity and seismic data suggest that the long-wavelength gravity anomalies arise due

to Moho-depth variations caused by flexing of the Indian lithosphere (Tiwari et al. 2006). Flexural model (e.g., Hetényi et al. 2006) explains the base of the foreland Indo-Gangetic basin and crustal thickness variations that corroborate with the results of receiver function analysis. Considering that long-wavelength gravity anomalies are explained with flexural Moho and basement, we have first defined Moho depth and basement based on average effective elastic thickness (EET) of ~40 km with Moho depth of 36 km in the south of Ganga Basin (Krishna and Rao 2005). The initial densities of different layers are assigned based on the previous studies (Gansser 1981; Cattin et al. 2001; Tiwari et al. 2006; Hetényi et al. 2007). Our initial model geometry is similar in the depth range inferred from seismic, seismological studies (DMG 1990; Hauck et al. 1998; Schulte-Pelkum et al. 2005). We consider the densities of 2,300 kg/m³ for the Indo-Gangetic sediment (Gansser 1981); 2,450 kg/m³ for the Siwalik sediment; 2,670 kg/m³ for the Indian Basement rock, Lesser, and Greater Himalaya formations; 2,900 and 3,270 kg/m³ for the Indian Lower Crust and Upper Mantle (Cattin et al. 2001), respectively. Besides, the initial densities of Tethys sediment, Asian Crust, part of the Indian Upper Crust toward north below the Asian Crust, and part of the Indian Lower Crust toward north below the Asian Crust are taken as 2,650 and 2,870 kg/m³ (Tiwari et al. 2010), 2,740 kg/m³ (Hetényi et al. 2007), and 2,980 kg/m³. We consider a single-fault geometry system (i.e., MHT, a major shear zone) where all the MFT, MBT, and MCT terminate at depth (cf. Makovsky et al. 1996; Hauck et al. 1998; Bollinger et al. 2006). We find the best fit between the observed and computed gravity field for the effective elastic thickness of ~40–50 km of the northward converging lithosphere. The present procedure (Fig. 3) is based on an interactive forward modeling (Webring 1985), which calculates the gravity responses of the modeled geometries. The initial geometries and initial densities of different layers provide the initial rms errors of 33 mgal for modeling along the profile AA' and 30 mgal along BB', respectively. The fit between observed and calculated gravity is compared through successive iterations, and the best fit is selected for the improved model. Finally, the rms error values reduce to 5.59 mgal and 7.41 mgal for profiles AA' and BB' for the optimum models (Figs. 4, 5). It is well known that Bouguer anomalies are combined effect of lateral density heterogeneities beneath reference level (in the present study, mean sea level, MSL) and anomalies due to departure of lithological densities from the reduction density (2.67 gm/cc) above reference level. The second component is small particularly over low-lying flat region; however, it is considerable in the regions like Himalaya. To overcome this problem, we have used density contrast with respect to 2,670 kg/m³ for the layers above MSL.

Fig. 3 Flowchart illustrating the path followed for gravity modeling

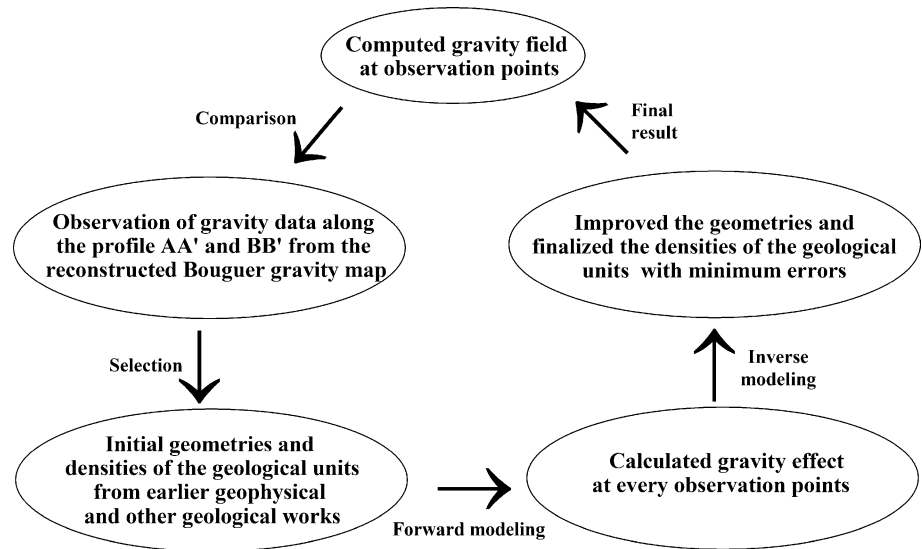
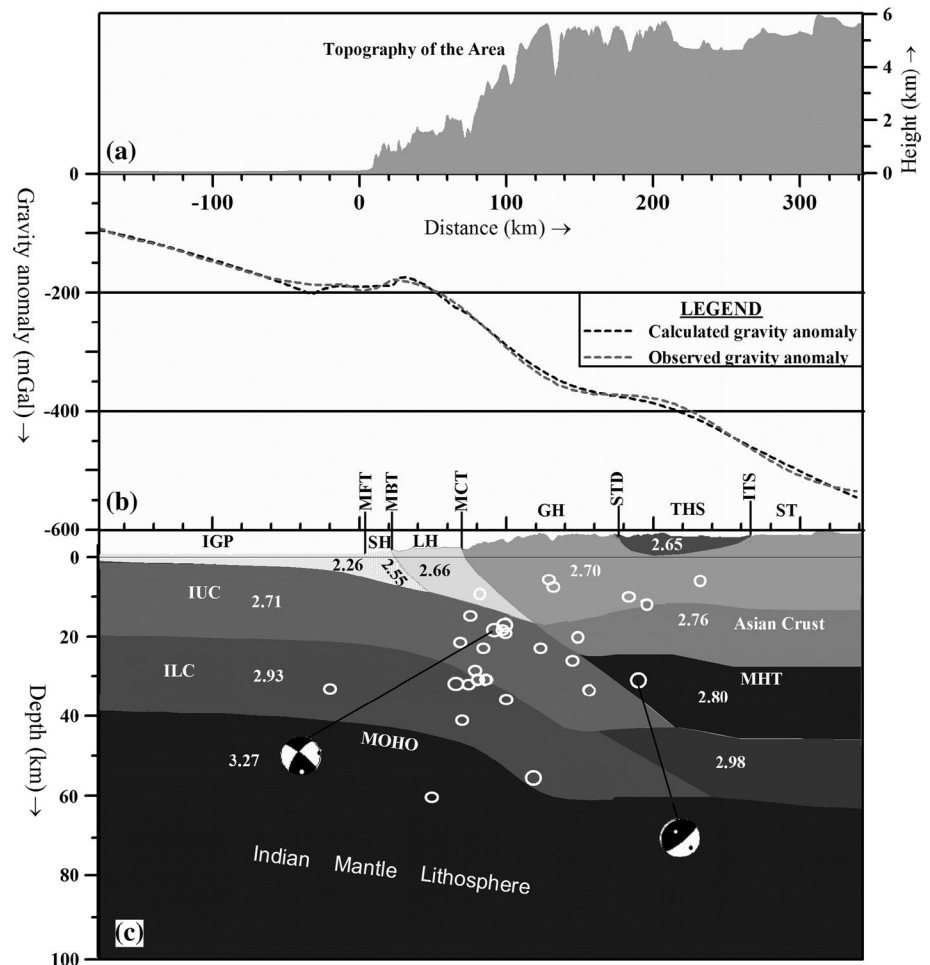


Fig. 4 Plot showing the 2D gravity modeling with topography along profile AA' for Nepal Himalaya. Plot at the *top* illustrates the topography of the area along AA' compiled from GTOPO 30, a global digital elevation model with a horizontal grid-spacing of 30 arc s (a). Plot at the *mid* illustrates a comparison between observed and computed Bouguer gravity anomalies along the profile (b). Lower plot (c) represents the 2D gravity density model. Hypocenter of 28 earthquake events and 2 focal mechanisms are also shown in the section of the model

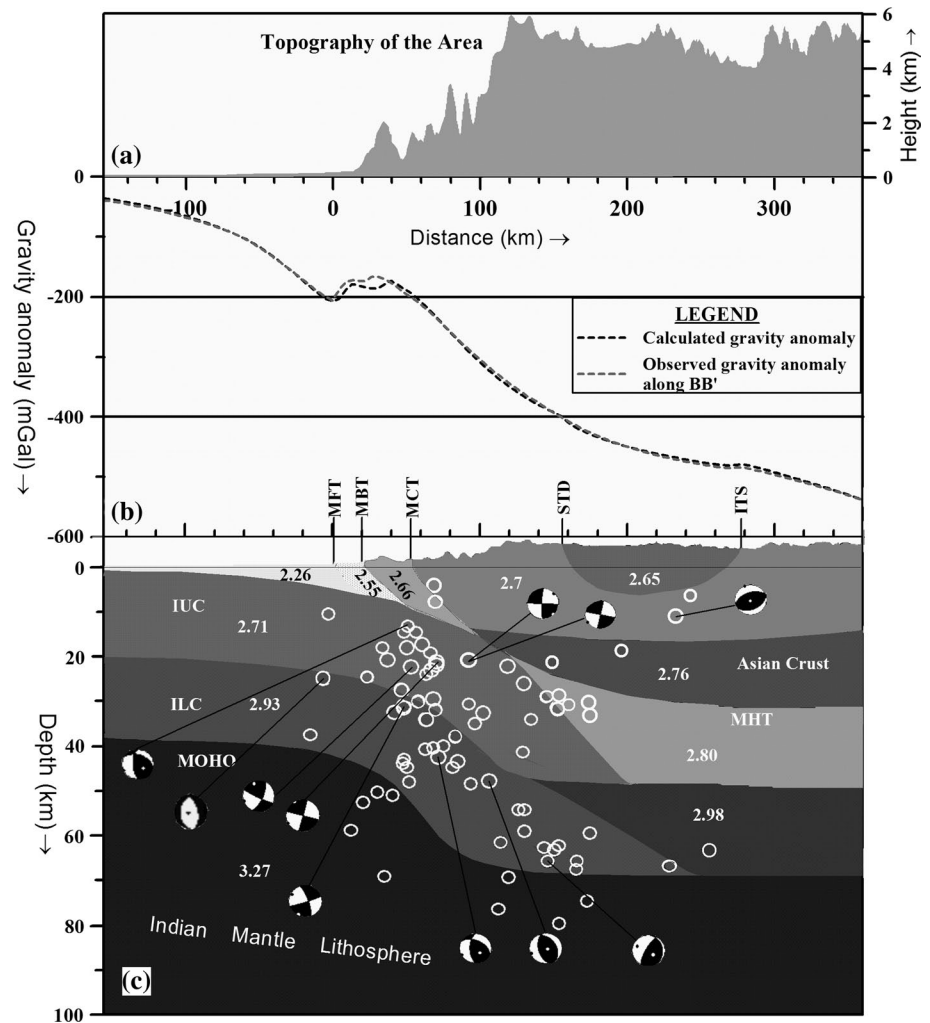


Finite-element modeling

Finite-element modeling for quantitative estimates of regional and local tectonic stress fields within the

lithosphere is an important tool for analyzing the lithospheric deformation (Artyushkov et al. 1996). In view of this, several workers (Willett et al. 1993; Beaumont et al. 1994; Sassi and Faure 1997; Mikhailov et al. 2002;

Fig. 5 Plot showing the 2D gravity modeling with topography along profile BB' for Sikkim–Darjeeling Himalaya. Plot at the top illustrates the topography of the area along AA' compiled from GTOPO 30, a global digital elevation model with a horizontal grid-spacing of 30 arc seconds (a). Plot at the mid illustrates a comparison between observed and computed Bouguer gravity anomalies along the profile (b). Lower plot (c) represents the 2D gravity density model. Hypocenter of 86 earthquake events and 11 focal mechanisms are also shown in the section of the model



Chamlagain and Hayashi (2004) have applied numerical modeling for understanding faulting and resulting geodynamics. Singh et al. (1990) modeled a cross section extending from the Ganga Plain to the Tibetan Plateau, aiming to simulate earthquake activity using force rather than displacement boundary conditions. Vergne et al. (2001) preferred 2D finite-element model consisting of different rheological layering of the continental lithosphere. Using the distinct-element method (Cundall 1990) or the finite-element method (Zienkiewicz and Taylor 1989, 1991), Sassi and Faure (1997) computed stress pattern, which depends on the boundary conditions, the presence of large-scale discontinuities, and/or contrasting mechanical properties of the constitutive rocks. Wang and Shi (1982) proposed through 2D finite-element modeling that the Himalaya is dynamically supported. Berger et al. (2004) used the ADELI 2D finite-element code (Hassani 1994; Hassani et al. 1997) to simulate the interseismic deformation in the three distinct western, central, and eastern Nepal blocks. They considered three geological domains along each

profile, Indian crust, Tibetan crust, and upper mantle. The rheologies of these three blocks were assumed to be homogeneous along the models and similar for eastern, central, and western Nepal.

In the present study, we perform finite-element modeling on two 2D vertical sections of the underthrust Indian and overthrust Asian lithospheres, along the profiles AA' (~520 km long) and BB' (~515 km long) in the Nepal Himalaya and Sikkim–Darjeeling Himalaya. The vertical section is divided into 11 different layers following the works of Owens and Zandt (1997), Cattin et al. (2001), Tiwari et al. (2006), Hetényi et al. (2007), and Hammer et al. (2013). Meshing is done through reconstruction of 1,039 nodes and 1,774 triangular elements along profile AA' for the Nepal Himalaya, and 993 nodes and 1,746 triangular elements along the profile BB' for the Sikkim–Darjeeling Himalaya. To understand the localized deformation vis-à-vis displacements, one should have the knowledge of rheology of the constituent rocks. The rock rheology has a significant influence on the occurrences of earthquakes as

Table 1 Physical parameters for different crustal units used for the gravity and finite-element modeling

Layer nos.	Crustal layers/ geological units	Density (kg/m ³)	Poisson's ratio (ν)	Young's modulus (E in GPa)	Cohesion coefficient (MPa)	Frictional coefficient
1	Indo-Gangetic plain	2,260	0.258	22.7	8	0.57
2	Sub-Himalaya	2,550	0.258	25.6	12	0.84
3	Lesser Himalaya	2,660	0.258	26.7	15	0.84
4	Higher Himalaya	2,700	0.257	27	18	0.84
5	Tethys Himalaya	2,650	0.258	26.6	17	1
6	Asian crust	2,760	0.258	61	10	0.12
7	Southern part of Indian upper crust	2,710	0.258	60	10	0.57
8	Northern part of Indian upper crust	2,800	0.258	62.1	10	0.57
9	Southern part of Indian lower crust	2,930	0.257	86.7	10	0.57
10	Northern part of Indian lower crust	2,980	0.257	88.2	10	0.57
11	Mantle	3,270	0.247	189.9	10	0.57

well as the source dynamics/kinematics (Watts and Burov 2003; Khan and Chakraborty 2009). The rock rheologies involving density, Poisson's ratio, Young's modulus, angle of friction, and cohesive strength of the rock are used for elastic modelling. The other parameters like cohesion coefficient (c) and frictional angle (φ) have been taken from the studies of Cattin et al. (2001), Hetényi et al. (2006), and Clark (1966). The improved density parameters of the different rock layers, achieved through the present gravity modeling (Figs. 4, 5, Table 1), are used for the finite-element modeling. The rock properties vary laterally as well as vertically. For the simplicity of computation, the whole models are divided into 11 layers and each layer has been assigned with distinct rock properties. The other parameters such as Poisson's ratio (ν) and Young's modulus (E) have been computed using the following equations (Timosenko and Goodier 1970; Shearer 1999).

$$\nu = \frac{(V_p^2 - 2V_s^2)}{2(V_p^2 - V_s^2)} \quad (1)$$

where seismic wave velocities, V_p (P-wave) and V_s (S-wave), were taken from the studies of Cotton et al. (1996) and Khattri et al. (1995).

$$E = \rho V_p^2 \frac{(1 + \nu)(1 - 2\nu)}{(1 - \nu)} \quad (2)$$

where ρ is the density. The values of densities for different layers are taken from Table 1.

Boundary conditions play important role in simulating the tectonic processes. In order to get the real situation, we apply the reasonable boundary conditions to represent the present-day kinematics in the Himalayan fold-and-thrust belt. The boundary conditions are illustrated in Fig. 6a, b under the present finite-element modeling. In

both the models, the upper surface is free to move in all directions. The lower section of the northern boundary below the MHT is fixed horizontally (cf. open circles, Fig. 6) for understanding the deformation caused by resistive forces along the Himalaya (Richardson 1992; Copley et al. 2010). The force balance calculations for the pre- and post-collision configurations under application of forces on the edges of the plate and the tractions on the base of the plate (Copley et al. 2010) showed that the resistive force induced by mountain building in the Himalaya–Tibet area is $\sim 5\text{--}6 \times 10^{12}$ N/m. We therefore impart an amount of 6×10^{12} N/m force, instead of displacement, on the frontal vertical part of the section (cf. arrows in Fig. 6), which is equivalent to the resistive force caused by the Himalayan–Tibet system to the Indian plate (Copley et al. 2010).

Results and discussion

The varying degrees of tectonic loading and flexure are imaged by earthquake receiver function analysis (Hetényi et al. 2006; Rai et al. 2006), seismicity studies (Seeber and Armbruster 1981; Ni and Barazangi 1984), magnetotelluric (MT) experiments (Chen et al. 1996; Lemonnier et al. 1999; Unsworth et al. 2005; Arora et al. 2007), seismic profiling (DMG 1990), INDEPTH (Zhao et al. 1993; Nelson et al. 1996; Hauck et al. 1998; Alsdorf et al. 1998), HIMNT experiment (Schulte-Pelkum et al. 2005), and gravity modeling (Lyon-Caen and Molnar 1985; Cattin et al. 2001; Banerjee and Prakash 2003; Jordan and Watts 2005; Tiwari et al. 2006) in different parts of the Himalaya. Invariably, different studies are in agreement with the three interfaces, the Moho, lower–upper crustal interface (Conrad discontinuity), and mid-crustal decollement (Hetényi et al. 2006). We summarize the gravity modeling results in Table 2 for depth distributions of these three different

Fig. 6 Plot showing the simplified geometries (after present gravity models) with boundary conditions for the 2D finite-element modeling for Nepal (a) as well as Sikkim–Darjeeling (b) Himalayas

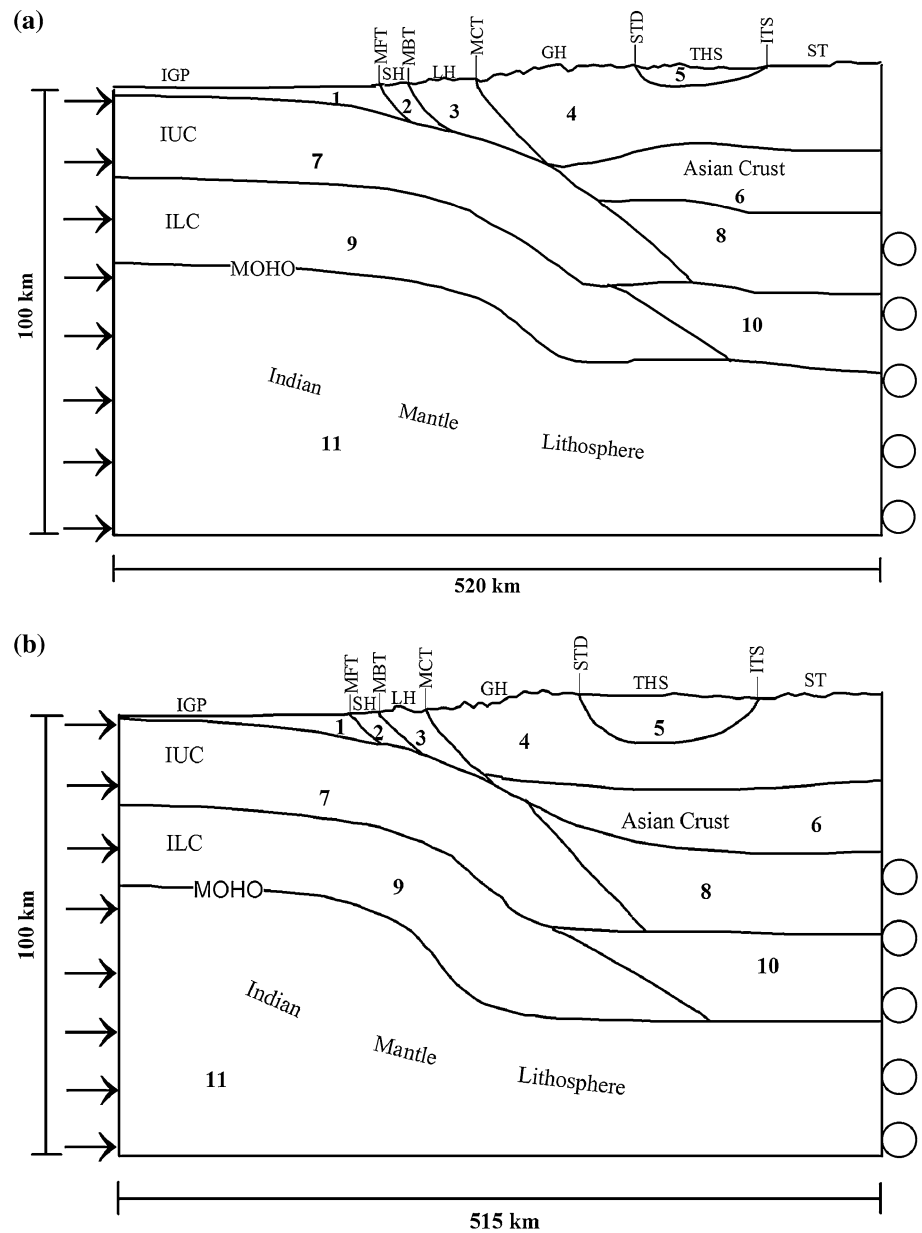


Table 2 Showing the depth variations in different crustal interfaces along profiles AA' and BB' below different crustal provinces in the Nepal and Sikkim–Darjeeling Himalayas

Crustal provinces	Nepal Himalaya				Sikkim–Darjeeling Himalaya			
	MHT	Conrad	Moho	No. of event	MHT	Conrad	Moho	No. of event
Indo-Gangetic plain	2–7	21–24	40–44	01	2–5	20–24	38–43	03
Siwalik Himalaya	7–9	24–26	44–45	00	5–7	24–26	43–46	04
Lesser Himalaya	9–15	26–32	45–51	04	7–11	26–33	46–55	19
Higher Himalaya	15–33	32–51	51–67	19	11–29	33–53	55–74	48
Tethys Himalaya	33–38	51–52	67–68	04	29–38	53–55	74–75	12
Southern Tibet	38–40	52–54	68–69	–	38–39	55	75	–

interfaces beneath the different crustal provinces along the south–north transects AA' and BB' for the Nepal and Sikkim–Darjeeling Himalayas. We note that the northward

continuity of the MHT, Conrad (boundary between IUC and ILC), and Moho is more or less gentle and similar beneath the Indo-Gangetic plain, Siwalik Himalaya, and

Lesser Himalaya. However, a sharp change in dips of all these crustal features is quite apparent further north beyond the Lesser Himalaya. Dip changes are reduced significantly from the Tethys Himalaya toward southern Tibet. We also critically examine the distribution of seismicity below different tectonic provinces and note a clear distinction of seismicity concentration. Greater Himalaya in both Nepal and Sikkim–Darjeeling records maximum concentration of seismic events. Another important feature is the shallower Moho of 40–44 km in Nepal and 38–43 km in Sikkim–Darjeeling beneath the Gangetic alluvium increases beyond the Lesser Himalaya and attains ~69 km in Nepal and ~75 km in Sikkim–Darjeeling beneath the southern Tibet (Figs. 4, 5), suggesting a locus of flexural loading on the Indian crust beneath the Greater Himalaya. A relative assessment clearly demonstrates a higher concentration of seismicity (i.e., 48 events) beneath the Greater Himalaya of Sikkim–Darjeeling than the Nepal Himalaya (i.e., 19 events). We thus find an excellent correlation between the zone of sharp bending of the descending Indian lithosphere and the maximum concentration of seismicity. This is possibly indicating the highest degree of deformation within the sharp flexing zone of the converging lithosphere.

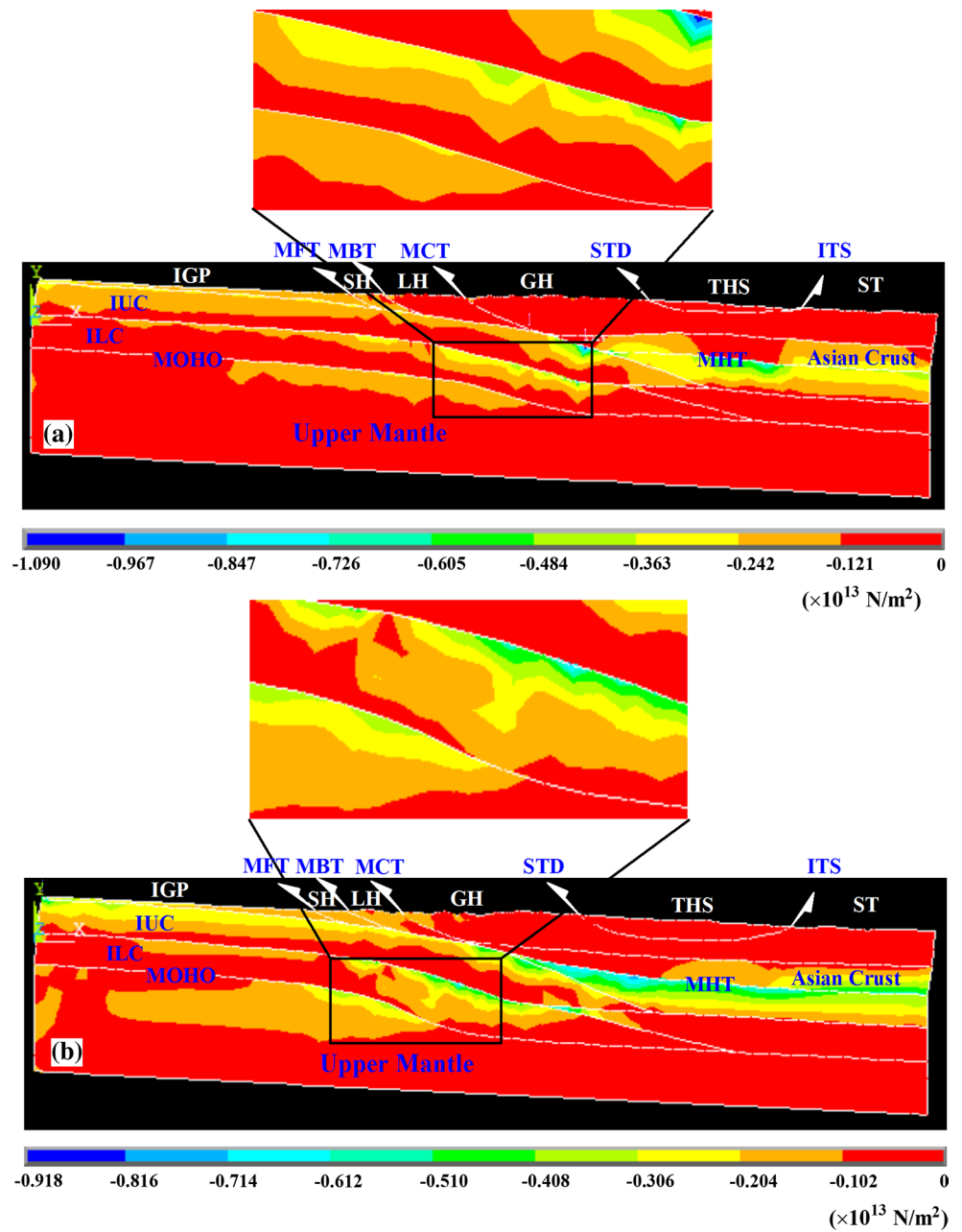
During finite-element modeling, a series of model calculations have been carried out, but only representative models are illustrated here. The computed stress fields and related faulting processes have been assessed through contouring of maximum compressive stress (σ_1) (Fig. 7a, b) and minimum compressive stress (σ_3) (Fig. 8a, b). We invariably note a zone of maximum compression ($\sim 10^{13}$ Pa) all along the northern part of the MHT (Fig. 7a, b). This higher compressive zone of one order more is abruptly terminated to the south of the Greater Himalaya. It was also noted that the compressive stress fields are more dominated within the different layers, and the relatively less compressive stress fields are distributed laterally in different layers of the Nepal Himalaya, while the bending zone of the converging lithosphere in Sikkim–Darjeeling Himalaya documents southwesterly distributed compressive stress field. The distribution of moderate ($\sim 3.3 \times 10^{12}$ Pa) compressive stress field is also found at the shallower part near the Indo-Gangetic plain. Figure 8a, b shows the distribution of minimum compressive stress field within the converging lithosphere. Although the minimum compressive stress fields are mainly confined near the upper surface of different layers around the bending portion of the descending Indian lithosphere, the minimum compressive stress is distributed laterally in Nepal Himalaya (Fig. 8a). Here, another important observation is that the magnitude of minimum compressive stress is nearly half of the maximum compressive stress.

Microseismicity survey in Nepal Himalaya shows that the seismic belt follows approximately the front of the

Greater Himalaya and especially more concentrated in eastern and far western Nepal. The earthquakes are generally shallower, clustered at a depth range of 10–20 km (Pandey et al. 1999; Kayal 2001). Based on the microseismicity survey in Sikkim–Darjeeling Himalaya, De (2000), Kayal (2001), Monsalve et al. (2006), and Hazarika et al. (2010) reported that the higher concentration of earthquakes is noted to the north of the MBT without following any particular trend. In addition, Kayal (2001) observed the earthquakes occurring predominantly below the plane of detachment and proposed that the MBT is seismogenic up to the mantle in the Sikkim Himalaya. While the present study reveals that the seismic activity is more concentrated right within the converging Indian lithosphere beneath the Greater Himalaya (Figs. 4, 5) with a significant distribution in the uppermost part of the Indian mantle lithosphere. Kayal (2001) and Nábelek et al. (2009) also identified active deformation within the upper mantle in the Sikkim Himalaya. Besides, the occurrence frequency or the incidences of numbers of earthquakes in Sikkim–Darjeeling section are quite unusual, whereas the Nepal Himalaya documents less seismic activity. Figure 9 illustrates the variation in dip-angle of the Moho boundary of the penetrating Indian lithosphere. A noteworthy change in dip-angles (e.g., $\sim 6^\circ$ – 8°) of the Moho boundary beyond MCT, particularly, beneath the Greater Himalaya is identified from Nepal to Sikkim–Darjeeling sectors. We thus may anticipate that the higher seismicity concentration might be caused by the increasing bending of the Indian lithosphere below the Sikkim–Darjeeling Himalaya. This was also appreciated in the literature (Conrad and Hager 1999) that ~60 % of energy dissipation occurs through the bending portion (flexing zone) of the subducting slab. It was noted that the hypocenters of the mega-earthquake events coincide with the zone of flexing (cf. Khan and Chakraborty 2005, 2009; Khan 2011; Khan et al. 2012) where the descending lithosphere takes a sharp change in inclination to reach into the deeper level. It was estimated that the maximum bending stress in the descending oceanic lithosphere at the subduction margins is about an order of magnitude larger than the maximum strength of the oceanic lithosphere (Kohlstedt et al. 1996; Conrad and Hager 1999); only 10 % of the elastic bending stress is supported without deformation, and the remaining stress is relieved in the form of seismicity by fracturing of rocks (e.g., Turcotte and Schubert 1982). Recent works of Singh et al. (2008), Khan and Chakraborty (2009), Khan (2011), and Khan et al. (2012) on the source dynamics and localization of hypocenter of the 2004 off Sumatra mega event envisage its association with the uppermost part of the mantle and advocate its intraplate origin.

Focal mechanisms of moderate magnitude earthquakes reveal that the sharp bending section of the lithosphere is

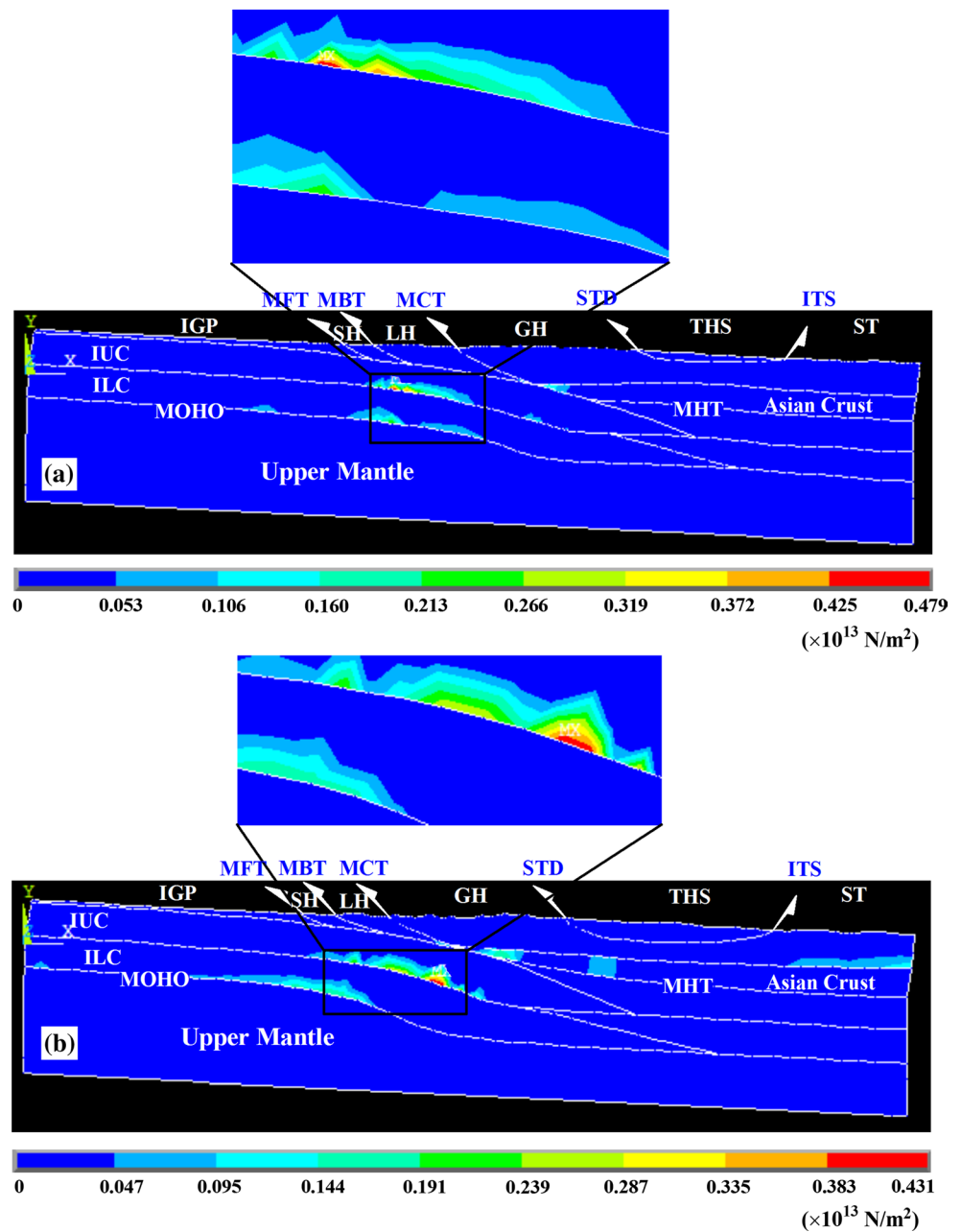
Fig. 7 Contour plot illustrates the variations in the maximum compressive stress fields (σ_1) for Nepal (a) and Sikkim–Darjeeling (b) Himalayas. Note the confinement of σ_1 right within the layers



associated with both strike-slip and thrust-dominated movements, and shear planes of most of these events are more or less parallel with the interfaces of the different crustal layers. Another significant observation is the dominant right-lateral shear movements operative in the crust part of the converging lithosphere, which is possibly controlled by either local or regional changes in plate obliquities (Liu et al. 1995). These typical features might be accounting an accommodation of crustal packages along both orthogonal and parallel with the arc of the Himalaya. We thus propose that the deformation is more dominant within the sharp bending zone than other parts of the converging lithosphere, and the lateral shearing between crustal blocks

is presumably constrained by the obliquity of the plate. It was noted that the motions following the occurrences of moderate-to-large earthquake events in an oblique convergent margin are generally partitioned into trench-parallel shear component and trench perpendicular subduction component (Fitch 1972; Ben-Menahem et al. 1974; McCaffrey 1992, 1996; Ishii et al. 2005; Lay et al. 2005; Khan 2005; Khan et al. 2010). McCaffrey and Nabalek (1998) interpreted the right-lateral strike-slip fault motion on the Karakoram–Jiali fault zone and the east–west extension on north-trending normal faults, and the radial vergence slips in the Himalayas are all due to basal shear caused by the obliquely converging Indian plate beneath the Tibet. The

Fig. 8 Contour plot illustrates the variations in the minimum compressive stress fields (σ_3) for Nepal (a) and Sikkim–Darjeeling (b) Himalayas. Note the distribution of σ_3 along the upper surfaces of different layers



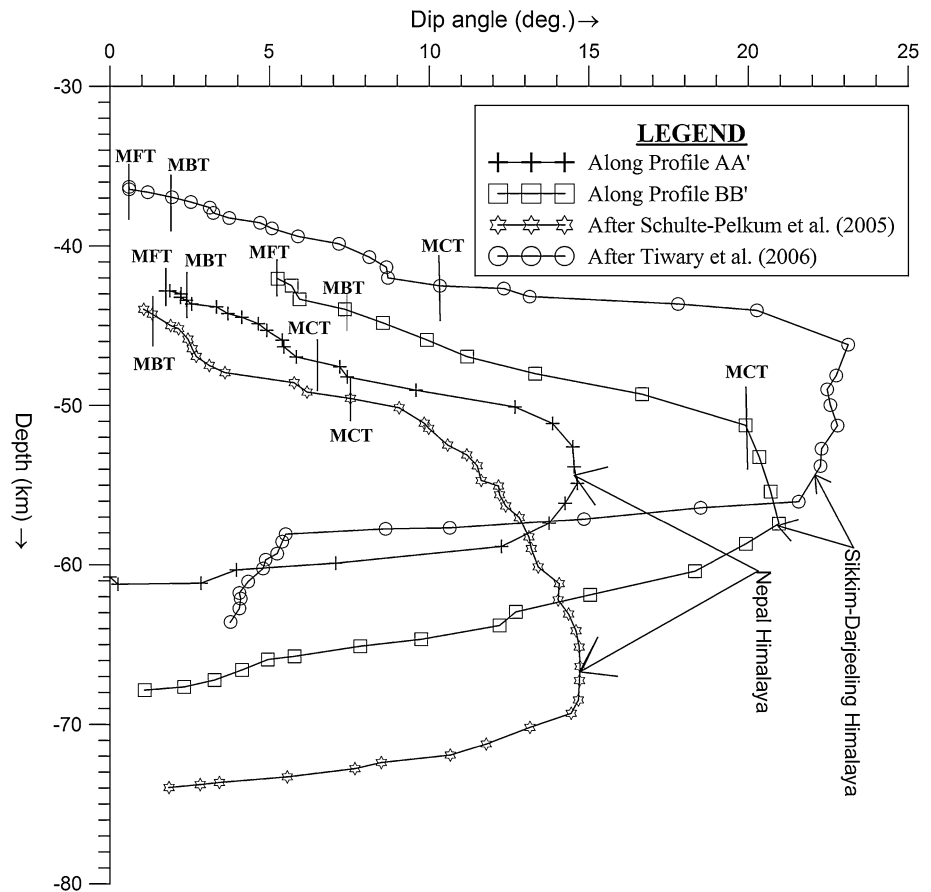
fluids at the mid-crustal depths surrounding MHT (Gokarn et al. 2002; Spratt et al. 2005; Unsworth et al. 2005; Patro and Harinarayan 2009) might be facilitating the slips along both orthogonal and parallel to the Himalayan arc.

Conclusions

Although the converging Indian lithosphere takes a sharp downward turn beneath the Greater Himalaya, relatively more steepening Moho boundary is identified through gravity modeling beneath the Sikkim–Darjeeling Himalaya.

This is likely correlated with higher seismicity concentration for this region. Further, a significant distribution of seismicity in the upper-most part of the mantle clearly shows its higher degree of deformation. It is also apparent from the finite-element modeling that the maximum compressive stress field is more confined right within the bending zone of the penetrating Indian lithosphere beneath the Greater Himalaya. We thus propose that the sharp bending zone of the converging Indian lithosphere is the nodal area of stress concentration and recording maximum deformation. Amplitude of estimated stresses might change due to uncertainties in the several parameters utilized to compute

Fig. 9 Plot showing the variations in dip-angles of Moho boundaries with depth along profiles AA', BB', XX', and YY', respectively. All profiles are shown in Fig. 2. Note the change in dip-angles of $\sim 6^\circ$ – 8° between sections of Nepal and Sikkim–Darjeeling Himalayas



the stresses; however, the pattern would remain same, and the inferences drawn from our studies remain valid.

We find dominant right-lateral shear motion in the crustal blocks of the Indian lithosphere and thrust-dominated movements orthogonal to the strike of the Himalaya. The strike-parallel components of motions of the converging Indian plate against the southern part of the Asian plate are presumably motivating the shear motion, and the strike-perpendicular components driving the radial vergence slips. The Indian plate obliquity is increasing both toward east and west of the Nepal Himalaya, and might be intrinsically related with the degree of arc-parallel shear motion. We thus may expect maximum lateral shearing of crustal blocks toward the termini of the Himalaya, where the Indian plate obliquity reaches its highest values.

Acknowledgments The first author is grateful to the Director, Indian School of Mines, Dhanbad, for partial financial support to carry out the present work. Partial financial benefit from the Ministry of Earth Sciences, Govt. of India, New Delhi, India, is also thankfully acknowledged. First author is also thankful to Gautam Kumar Nayak, Scientist, National Geophysical Research Institute, Hyderabad, India, for his critical suggestions during gravity modelling. The authors are thankful to Gautam Gupta and other anonymous reviewer for excellent suggestion, which has improved the manuscript.

References

- Acharya SK, Ray KK (1977) Geology of the Darjeeling–Sikkim Himalaya. In: Guide to excursion no. 3, fourth international Gondwana Symposium (Calcutta), Geological Survey of India, pp 1–25
- Alsdorf D, Makovsky Y, Zhao W, Brown LD, Nelson KD, Klemperer S, Hauck M, Ross A, Cogan M, Clark M, Che J (1998) INDEPTH (International Deep Profiling of Tibet and the Himalaya) multichannel seismic reflection data: description and availability. *J Geophys Res* 103(26):993–999
- Ansari MA, Khan PK (2013) Occurrences of damaging earthquakes between the Himachal and Darjeeling Himalayas: tectonic implications. *Acta Geophysica* (accepted)
- Argand E (1924) La tectonique de l'Asie. *Int Geol Congr Rep Sess* 13:170–372
- Arora BR, Unsworth MJ, Rawat G (2007) Deep resistivity structure of the northwest Indian Himalaya and its tectonic implications. *Geophys Res Lett* 34(4). doi:10.1029/2006GL029165
- Artyushkov EV, Baer MA, Morner NA (1996) An independence of subsidence of the Earth crust and mountains building in Carpathians from thrust loading. *Trans (Doklady) Russ Acad Sci/Earth Sci Sec* 346:103–107
- Banerjee P, Prakash S (2003) Crustal configuration in north western Himalaya from gravity measurements along Kiratpur-Leh-Panamik transect. *Geol Soc India* 61:529–539
- Bapat A, Kulkarni RC, Guha SK (1983) Catalogue of earthquakes in India and neighborhood—from historical period up to 1979. Indian Society of Earthquake Technology, Roorkee

- Beaumont C, Fullsack P, Hamilton J (1994) Styles of crustal deformation in compressional orogens caused by subduction of the underlying lithosphere. *Tectonophysics* 232:119–132
- Ben-Menaheem A, Aboodi E, Schild R (1974) The source of great Assam earthquake—an interplate wedge motion. *Phys Earth Planet Inter* 9:265–289
- Berger A, Jouanne F, Hassani RD, Mugnier JL (2004) Modelling the spatial distribution of the present-day deformation in Nepal: how cylindrical is the main Himalayan thrust in Nepal? *Geophys J Int* 156:94–114
- Besse J, Courtillot V, Pozzi JP, Westphal M, Zhou YX (1984) Palaeomagnetic estimates of crustal shortening in the Himalayan thrusts and Zangbo suture. *Nature* 311:621–626
- Bilham R, Gaur VK (2000) Geodetic contributions to the study of seismotectonics in India. *Curr Sci* 79(9):1259–1269
- Bollinger L, Henry P, Avouac JP (2006) Mountain building in the Nepal Himalaya: thermal and kinematic model. *Earth Planet Sci Lett* 244:58–71
- Burbank DW, Beck RA, Mulder T (1996) The Himalayan foreland basin. In: Yin A, Harrison TM (eds) *The tectonics of Asia*. Cambridge University Press, New York, pp 149–188
- Burg JP, Chen GM (1984) Tectonics and structural formation of southern Tibet, China. *Nature* 311:219–223
- Cattin R, Avouac JP (2000) Modeling mountain building and the seismic cycle in the Himalaya of Nepal. *J Geophys Res* 105:13389–13407
- Cattin R, Martelet G, Henry P, Avouac JP, Diament M, Shaky TR (2001) Gravity anomalies, crustal structure and thermo-mechanical support of the Himalaya of Central Nepal. *Geophys J Int* 147:381–392
- Chamlaigain D, Hayashi D (2004) Numerical simulation of fault development along NE–SW Himalayan profile in Nepal. *J Nepal Geol Soc* 29:1–11
- Chandra U (1978) Seismicity, earthquake mechanisms and tectonics along the Himalayan mountain range and vicinity. *Phys Earth Planet Inter* 16:109–131
- Chen L, Booker JR, Jones AG, Wu N, Unsworth MJ, Wei W, Tan H (1996) Electrically conductive crust in southern Tibet from in depth MT surveying. *Sci* 274:1694–1696
- Clark SP Jr (1966) *Handbook of physical constants*. Geol Soc Am Mem 97:1–587
- Conrad CP, Hager BH (1999) Effects of plate bending and fault strength at subduction zones on plate dynamics. *J Geophys Res* 104:17551–17571. doi:10.1029/1999JB900149
- Copeland P, Harrison TM, Yun P, Kidd WSF, Roden M, Zhang Y (1995) Thermal evolution of the Gangdese batholith, southern Tibet: a history of episodic unroofing. *Tectonics* 14:223–236
- Copley A, Avouac JP, Royer JY (2010) India-Asia collision and the Cenozoic slowdown of the Indian plate: Implications for the forces driving plate motions. *J Geophys Res* 115. doi:10.1029/2009JB006634
- Cotton F, Campillo M, Deschamps A, Rastogi B (1996) Rupture history and seismotectonics of the 1991 Uttarkashi Himalaya earthquake. *Tectonophysics* 258:35–51
- Cundall RA (1990) Numerical modelling of jointed and fractured rock. In: Rossmannith HR (ed) *Mechanics of jointed and faulted rock*. Balkema, Rotterdam, pp 11–28
- Dasgupta S, Mukhopadhyay M, Nandy DR (1987) Active transverse features in the central portion of the Himalaya. *Tectonophysics* 136:255–264
- De R (2000) A microearthquake survey at the MBT zone: Sikkim Himalaya. *J Geophys Res* 21:1–8
- Debon F, LeFort P, Sheppard SMF, Sonet J (1986) The 4 plutonic belts of the Trans Himalaya and Himalaya—a chemical, mineralogical, isotopic, and chronological synthesis along a Tibet–Nepal section. *J Petrol* 27:219–250
- DeMets C, Gordon RG, Argus DF, Stein S (1990) Current plate motions. *Geophys J Int* 101:425–478
- DeMets C, Gordon RG, Argus DF, Stein D (1994) Effect of recent revisions to the geomagnetic reversal time scale and estimates of current plate motions. *Geophys Res Lett* 21:2191–2194
- DMG (1990) *Exploration opportunities in Nepal*. Department of Mines and Geology, Kathmandu, p 32
- Duncan C, Masket J, Fielding E (2003) How steep are the Himalaya? Characteristics and implications along-strike topographic variations. *Geology* 31:75–78
- Fitch TJ (1972) Plate convergence, transcurrent faults and internal deformation adjacent to southeast Asia and the western Pacific. *J Geophys Res* 77:4432–4460
- Forste C et al (2008) The Geo Forschungs Zentrum Potsdam/Groupe de Recherche de Geodesie Spatiale satellite-only and combined gravity field models: EIGEN-GL04S1 and EIGEN-GL04C. *J Geod* 82(6):331–346. doi:10.1007/s00190-007-0183-8
- Gaetani M, Garzanti E (1991) Multicyclic history of the northern India continental margin (northwestern Himalaya). *Am Assoc Petrol Geol Bull* 75:1427–1446
- Gahalaut VK, Kundu B (2012) Possible influence of subduction ridges on the Himalayan arc and on the ruptures of great and major Himalayan earthquakes. *Gondwana Res* 21:1080–1088
- Gansser A (1964) *Geology of the Himalaya*. Intersci Pub, London, pp 1–273
- Gansser A (1981) The Geodynamic history of the Himalaya. In: Gupta HK, Delany FM (eds) *Zagros, Hindu-Kush, Himalaya. Geodynamic evolution*. Am Geophys Union, Geodynamics Series 3, Washington, DC, pp 111–121
- Gokam SG, Gupta G, Rao CK, Selvaraj C (2002) Electrical structure across the Indus Tsangpo suture and Shyok suture zones in NW Himalaya using magnetotelluric studies. *Geophys Res Lett* 29(8). doi:10.1029/2001GL014325
- Hammer P, Berthet T, Hetényi G, Cattin R, Drukpa D, Chopel J, Lechmann S, Le Moigne N, Champollion C, Doeringer E (2013) Flexure of the India Plate underneath the Bhutan Himalaya. *Am Geophys Union* 40(16):4225–4230. doi:10.1002/grl.50793
- Hassani R (1994) *Modélisation numérique de la déformation des systèmes géologiques* (Ph.D. Thesis). University of Montpellier II
- Hassani R, Jongmans D, Chéry J (1997) Study of plate deformation and stress in subduction processes using two-dimensional numerical models. *J Geophys Res* 102:17951–17965
- Hauck ML, Nelson KD, Brown LD, Zhao W, Ross AR (1998) Crustal structure of the Himalaya orogen at ~90° east longitude from INDEPTH deep reflection profiles. *Tectonics* 17:481–500
- Hazarika P, Kumar MR, Sriyjanthi G, Raju PS, Rao PN, Srinagesh D (2010) Transverse tectonics in the Sikkim Himalaya: evidence from seismicity and focal-mechanism data. *Bull Seismol Soc Am* 100(4):1816–1822. doi:10.1785/0120090339
- Heim A, Gansser A (1939) Central Himalaya: geological observations of the swiss expedition 1936: Zürich, *Memoires de la Société Helvétique des Sciences Naturelles*, vol 73. Gebrüder Fretz, p 245
- Hetényi G, Cattin R, Vergne J, Nábělek JL (2006) The effective elastic thickness of the India Plate from receiver function imaging, gravity anomalies and thermomechanical modeling. *Geophys J Int* 167:1106–1118
- Hetényi G, Cattin R, Brunet F, Bollinger L, Vergne J, Nábělek JL, Diament M (2007) Density distribution of the India plate beneath the Tibetan plateau: geophysical and petrological constraints on the kinetics of lower-crustal eclogitization. *Earth Planet Sci Lett* 264:226–244
- Hirn A, Jobert G, Wittlinger G, Zhong-Xin X, En-Yuan G (1984) Main features of the upper lithosphere in the unit between the High Himalayas and the Yarlung Angbo Jiang suture. *Ann Geophys* 2:113–118

- Hodges KV (2000) Tectonics of the Himalayan and southern Tibet from two perspectives. *Geol Soc Am Bull* 112:324–350
- Hubbard MS, Harrison TM (1989) $^{40}\text{Ar}/^{39}\text{Ar}$ age constraints on deformation and metamorphism in the Main Central Thrust zone and in Tibetan Slab, eastern Nepal Himalaya. *Tectonics* 8:865–880
- Ishii M, Shearer PM, Houston H, Vidale JE (2005) Extent, duration and speed of the 2004 Sumatra–Andaman earthquake imaged by the hi-net array. *Nature* 435:933–936
- Jin Y, McNutt MK, Zhu YS (1996) Mapping the descent of Indian and Eurasian plates beneath the Tibetan Plateau from gravity anomalies. *J Geophys Res* 101:11275–11290
- Johnson MRW (2002) Shortening budgets and the role of continental subduction during the India–Asia collision. *Earth Sci Rev* 59:101–123
- Jordan TA, Watts AB (2005) Gravity anomalies, flexure and the elastic thickness structure of the India–Eurasia collisional system. *Earth Planet Sci Lett* 235:732–750
- Kayal JR (2001) Microearthquake activity in some parts of the Himalaya and the tectonic model. *Tectonophysics* 339:331–351
- Khan PK (2005) Variation in dip-angle of the Indian plate subducting beneath the Burma plate and its tectonic implications. *Int Geosci J* 9:227–234
- Khan PK (2011) Role of unbalanced slab resistive force in the 2004 off Sumatra mega earthquake ($M_w > 9.0$) event. *Int J Earth Sci* 100:1749–1758. doi:10.1007/s00531-010-0576-4
- Khan PK, Chakraborty PP (2005) Two-phase opening of Andaman Sea: a new seismotectonic insight. *Earth Planet Sci Lett* 229:259–271
- Khan PK, Chakraborty PP (2009) Bearing of plate geometry and rheology on shallow-focus mega thrust seismicity with special reference to 26 December 2004 Sumatra event. *J Asian Earth Sci* 34:480–491
- Khan PK, Mohanty S, Mohanty M (2010) Geodynamic implications for the 8 October 2005 North Pakistan earthquake. *Survey Geophys* 31:85–106. doi:10.1007/s10712-009-9083-1
- Khan PK, Chakraborty PP, Tarafder G, Mohanty S (2012) Testing the intraplate origin of mega-earthquakes at subduction margins. *Geosci Front* 3:473–481. doi:10.1016/j.gsf.2011.11.012
- Khan PK, Ansari MA, Mohanty S (2014) Earthquake source characteristics along the arcuate Himalayan belt: its tectonic implications. *J Earth Sys Sci* (accepted).
- Khattari KN (1987) Great earthquakes, seismicity gaps and potential for earthquakes along the Himalayan plate boundary. *Tectonophysics* 138:7:9–92
- Khattari KN, Anderson JG, Brune JN, Zeng Y (1995) Strong ground motion from the Uttarkashi, Himalaya, India, Earthquake: comparison of observations with synthetic using the composite source model. *Bull Seismol Soc Am* 85(1):31–50
- Klootwijk CT, Conaghan PJ, Powell CM (1985) The Himalayan arc: large-scale continental subduction, oroclinal bending, and back-arc spreading. *Earth Planet Sci Lett* 75:316–319
- Kohlstedt DL, Keppeler H, Rubie DC (1996) Solubility of water in the α , β and γ phases of $(\text{Mg}, \text{Fe})_2\text{SiO}_4$. *Contrib Miner Petrol* 123:345–357
- Krishna VG, Rao VV (2005) Processing and modelling of short-offset seismic refraction—coincident deep seismic reflection data sets in sedimentary basins: an approach for exploring the underlying deep crustal structures. *Geophys J Int* 163:1112–1122. doi:10.1111/j.1365-246X.2005.02792.x
- Lavé J, Avouac JP (2000) Active folding of fluvial terraces across the Siwaliks Hills, Himalayas of central Nepal. *J Geophys Res* 105:5735–5770
- Lay T, Kanamori H, Ammon CJ et al (2005) The great Sumatra–Andaman earthquake of 26 December 2004. *Science* 308:1127–1133
- Le Fort P (1975) Himalayas, the collided range: present Knowledge of the continental arc. *Am J Sci* 275:1–44
- Le Fort P (1986) Metamorphism and magmatism during the Himalayan collision. In: Coward MP, Ries AC (eds) *Collision tectonics*. *Geol Soc Lond Spec Publ* 19:159–172
- Lemonnier C, Marquis G, Perrier F, Avouac JP, Chitrakar G, Kafle B, Sapkota S, Gautam U, Tiwari D, Bano M (1999) Electrical structure of the Himalaya of Central Nepal: high conductivity around the mid-crustal ramp along the MHT. *Geophys Res Lett* 26:3261–3264
- Li C, Hilst RDV, Meltzer AS, Engdahl ER (2008) Subduction of the Indian lithosphere beneath the Tibetan Plateau and Burma. *Earth Planet Sci Lett* 274:157–168
- Liu X, McNally KC, Shen ZK (1995) Evidence for a role of the downgoing slab in earthquake slip partitioning at oblique subduction zones. *J Geophys Res* 100:15351–15372
- Long S, McQuarrie N, Tobgay T, Grujic D (2011) Geometry and crustal shortening of the Himalayan fold-thrust belt, eastern and central Bhutan. *Geol Soc Am Bull* 123:1427–1447. doi:10.1130/B30203.1
- Lyon-Caen H, Molnar P (1983) Constraints on the structure of the Himalaya from an analysis of gravity anomalies and a flexural model of the lithosphere. *J Geophys Res* 88:8171–8192
- Lyon-Caen H, Molnar P (1985) Gravity anomalies, flexure of the Indian plate, and the structure, support and evolution of the Himalaya and Ganga Basin. *Tectonics* 4:513–538
- Makel G, Walters J (1993) Finite-element analysis of the thrust tectonics: computer simulation of detachment phase and development of thrust faults. *Tectonophysics* 226:167–185
- Makovsky Y, Klemperer SL, Huang L, Lu D, Project INDEPTH Team (1996) Structural elements of the southern Tethyan Himalaya crust from wide-angle seismic data. *Tectonics* 15:997–1005
- McCaffery R (1996) Estimates of modern arc-parallel strain rates in fore arcs. *Geology* 24:27–30
- McCaffrey R (1992) Oblique plate convergence, slip vectors, and forearc deformation. *J Geophys Res* 97:8905–8915
- McCaffrey R, Nabalek J (1998) Role of oblique convergence in the active deformation of the Himalayas and Southern Tibet. *Geology* 26:691–694
- McQuarrie N, Robinson D, Long S, Tobgay T, Grujic D, Gehrels G, Ducea M (2008) Preliminary stratigraphic and structural architecture of Bhutan: implications for the along strike architecture of the Himalayan system. *Earth Planet Sci Lett* 272:105–117. doi:10.1016/j.epsl.2008.04.030
- Meigs AJ, Burbank DW, Beck RA (1995) Middle-late Miocene (>10 Ma) formation of the Main Boundary Thrust in the western Himalaya. *Geology* 23(5):423–462. doi:10.1130/0091-7613(1995)023<0423:MLMMFO>2.3.CO;2
- Mikhailov AV, Marin D (2001) An interpretation of the foF2 and hmF2 long-term trends in the framework of the geomagnetic control concept. *Ann Geophys* 19:733–748
- Mikhailov VO, Smolyaninov EI, Sebrier M (2002) Numerical modeling of neotectonic movements and the state of stressing the north Caucasus foredeep. *Tectonics* 21:1–14
- Molnar P (1983) Average regional strain due to slip on numerous faults of different orientations. *J Geophys Res* 88:6430–6432
- Molnar P (1984) Structure and tectonics of the Himalaya: constraints and implications of geophysical data. *Ann Rev Earth Planet Sci* 12:489–518
- Molnar P (1988) Continental tectonics in the aftermath of plate tectonics. *Nature* 335:131–137
- Molnar P, Tapponnier P (1978) Active tectonics of Tibet. *J Geophys Res* 83:5361–5369
- Monsalve G, Sheehan A, Schulte-Pelkum V, Rajaure S, Pandey MR, Wu F (2006) Seismicity and one dimensional velocity structure of the Himalayan collision zone: Earthquakes in the crust and upper mantle. *J Geophys Res* 111. doi:10.1029/2005JB004062

- Nábelek J, Hetényi G, Vergne J, Sapkota S, Kae B, Jiang M, Su HP, Chen J, Huang BS (2009) Underplating in the Himalaya-Tibet collision zone revealed by the Hi-CLIMB experiment. *Science* 325:1371–1374
- Nelson M, Humphrey W, Gursoy A, Dalke A, Kalé L, Skeel RD, Schulten K (1996) NAMD—a parallel, object-oriented molecular dynamics program. *J Supercomput Appl* 10:251–268
- Ni J, Barazangi M (1984) Seismotectonics of the Himalayan collision zone: geometry of the underthrusting Indian Plate beneath the Himalaya. *J Geophys Res* 89:1147–1163
- Owens TJ, Zandt G (1997) The implications of crustal property variations on models of Tibetan Plateau evolution. *Nature* 387:37–43
- Pandey MR, Tandukar RP, Avouac JP, Vergne J, Heritier Th (1999) Seismotectonics of the Nepal Himalaya from a local seismic network. *J Asian Earth Sci* 17:703–712
- Patriat P, Achache J (1984) India–Eurasia collision chronology has implications for crustal shortening and driving mechanism for plates. *Nature* 311:615–621
- Patro PK, Harinarayan T (2009) Deep geoelectric structure of the Sikkim Himalayas (NE India) using magnetotelluric studies. *Phys Earth Planet Int* 173:171–176. doi:10.1016/j.pepi.2008.10.011
- Pavlis NK, Holmes SA, Kenyon SC, Factor JK (2008) An earth gravitational model to degree 2160:EGM2008. Presented to EGU-2008, Vienna, Austria, April 2008
- Rai SS, Priestley K, Gaur VK, Mitra S, Singh MP, Searle M (2006) Configuration of the Indian moho beneath the NW Himalaya and Ladakh. *Geophys Res Lett* 33. doi:10.1029/2006GL026076
- Raiverman V (2000) Foreland Sedimentation in Himalayan Tectonic Regime: a relook at the orogenic processes. *Bishen Singh Mahendra Pal Singh, Dehradun* 378
- Rajendran CP, Rajendran K (2005) The status of central seismic gap: a perspective based on the spatial and temporal aspects of the large Himalayan earthquake. *Tectonophysics* 395:19–39
- Rao MBR (1973) The subsurface geology of the Indo-Gangetic plains. *J Geol Soc India* 14:217–242
- Richardson RM (1992) Ridge forces, absolute plate motions, and the intraplate stress field. *J Geophys Res* 97:11739–11749
- Robert X, Vander Beek P, Braun J, Perry C, Dubille M, Mugnier JL (2009) Assessing Quaternary reactivation of the Main Central thrust zone (central Nepal Himalaya): new thermochronologic data and numerical modelling. *Geology* 37(8):731–734
- Sanker D, Kapur N, Singh B (2002) Thrust-wedge mechanics and coeval development of normal and reverse faults in the Himalayas. *J Geol Soc* 137:1–34
- Sassi W, Faure JL (1997) Role of fault and layer interfaces on the spatial variation of stress regimes in basins: inferences from numerical modelling. *Tectonophysics* 266:101–119
- Sastri VV, Bhandari LL, Raju ATR, Datta AK (1971) Tectonics framework and subsurface stratigraphy of the Ganga basin. *J Geol Soc India* 12:232–233
- Schärer U, Xu RH, Allègre CJ (1984) U-Pb geochronology of Gangdese (Transhimalaya) plutonism in the Lhasa-Xigaze region, Tibet. *Earth Planet Sci Lett* 69:311–320
- Schelling D (1992) The tectonostratigraphy and structure of the eastern Nepal Himalaya. *Tectonics* 11:925–943
- Schelling D, Arita K (1991) Thrust tectonics, crustal shortening, and the structure of the far-eastern Nepal, Himalaya. *Tectonics* 10:851–862
- Schulte-Pelkum V, Monsalve G, Sheehan A, Pandey MR, Sapkota S, Bilham R, Wu F (2005) Imaging the Indian subcontinent beneath the Himalaya. *Nature* 435:1222–1225
- Searle MP, Windley BF, Coward MP, Cooper DJW, Rex AJ, Rex D, Tingdongs L, Xuchangs X, Jan MQ, Thakur VC, Kumar S (1987) The closing of Tethys and the tectonics of the Himalaya. *Bull Geol Soc Am* 98:678–701
- Seeber L, Armbruster J (1981) Great detachment earthquakes along the Himalayan arc and long-term forecasting. In: Simpson DW, Richards PG (eds) *Earthquake Prediction. An international review*, Am Geophys Univ, Maurice Ewing Series 4, pp 215–242
- Shearer PM (1999) *Introduction to seismology*. Cambridge University Press, Cambridge
- Singh RP, Li Q, Nyland E (1990) Lithospheric deformation beneath the Himalayan region. *Phys Earth Planet Int* 61:291–296
- Singh SC, Carton H, Tapponnier P, Hananto ND, Chauhan APS, Hartoyo D, Bayly M, Moeljopranoto S, Bunting T, Christie P, Lubis H, Martin J (2008) Seismic evidence for broken oceanic crust in the 2004 Sumatra earthquake epicentral region. *Nat Geosci* 1(11):777–781
- Spratt JE, Jones AG, Nelson KD, Unsworth MJ, INDEPTH MT Team (2005) Crustal structure of the India-Asia collision zone, southern Tibet, from INDEPTH MT investigations. *Phys Earth Planet Int* 150:227–237
- Tandon AN (1972) Anantnag earthquakes (Feb–April, 1967). *Ind J Meteorol Geophys* 23:491
- Thiede RC, Bookhagena B, Arrow Smith JR, Sobela ER, Streckera MR (2004) Climatic control on rapid exhumation along the Southern Himalayan Front. *Earth Planet Sci Lett* 222:791–806
- Timosenko SP, Goodier JN (1970) *Theory of elasticity*, 3rd edn. McGraw-Hill Book Company, London, pp 1–567
- Tiwari VM, Vyghreswara R, Mishra DC, Singh B (2006) Crustal structure across Sikkim, NE Himalaya from new gravity and magnetic data. *Earth Planet Sci Lett* 247:61–69
- Tiwari VM, Singh B, Arora K, Kumar S (2010) The potential of satellite gravity and gravity gradiometry in deciphering structural setting of the Himalayan Collision Zone. *Curr Sci* 99(12):1795–1800
- Turcotte DL, Schubert G (1982) *Geodynamics applications of continuum physics to geological problems*. Wiley, New York, p 450
- Unsworth MJ, Jones AG, Wei W, Marquis G, Gokarn SG, Spratt JE, INDEPTH MT Team (2005) Crustal rheology of the Himalaya and southern Tibet inferred from magnetotelluric data. *Nature* 438:78–81
- Valdiya KS (1976) Himalaya transverse faults and their parallelism with subsurface structures of North Indian planes. *Tectonophysics* 32:353–386
- Valdiya KS (1980) *Geology of kumaun lesser himalaya*. Wadia Institute of Himalayan Geology, p 291
- Valdiya KS (1988) Tectonics and evolution of the central sector of the Himalaya. *Philos Trans R Soc Lond A Math Phys Sci* 326:151–174
- Valdiya KS (1989) Trans-Himadri intracrustal fault and basement upwards south of the Indus–Tsangpo suture zone. In: Malinconico Jr LL, Lillie RJ (eds) *Tectonics of the Western Himalaya*. Special paper, *Geol Soc Am* 232:153–168
- Vanbrabant Y, Jongmans D, Hassani R, Bellono D (1999) An Application of Two-dimensional finite-element modeling for studying the deformation of the Variscan Fold-and-thrust belt (Belgium). *Tectonophysics* 309:141–159
- Vergne J, Cattin R, Avouac JP (2001) On the use of dislocations to model interseismic strain and stress build-up at the intracontinental thrust faults. *Geophys J Int* 47:115–162
- Verma RK, Kumar GVRK (1987) Seismicity and the nature of plate movement along the Himalayan arc, Northeast India and Arakan-Yoma: a review. *Tectonophysics* 134:153–175
- Wang C, Shi Y (1982) On the tectonics of the Himalaya and Tibet plateau. *J Geophys Res* 87:2949–2957
- Watts AB, Burov EB (2003) Lithospheric strength and its relationship to the elastic and seismogenic layer thicknesses. *Earth Planet Sci Lett* 213:113–131

- Webring M (1985) SAKI: A Fortran program for generalized linear inversion of gravity and magnetic profiles. Open-file report, U.S. Geological Survey, pp 85–122
- Willet SD, Beaumont C (1994) Subduction of Asian lithospheric mantle beneath Tibet inferred from models of continental collision. *Nature* 369:642–645. doi:[10.1038/369642a0](https://doi.org/10.1038/369642a0)
- Willet SD, Beaumont C, Fullsack P (1993) Mechanical model for the tectonics of doubly vergent compressional orogens. *Geology* 21:371–374
- Yin A (2006) Cenozoic tectonic evolution of the Himalayan orogen as constrained by along-strike variation of structural geometry, exhumation history, and foreland sedimentation. *Earth Sci Rev* 76:1–131
- Zhang Z, Klemperer S (2010) Crustal structure of the Tethyan Himalaya, southern Tibet: new constraints from old wide-angle seismic data. *Geophys J Int* 181:1247–1260
- Zhao W, Nelson K, Team PI (1993) Deep seismic reflection evidence for continental underthrusting beneath southern Tibet. *Nature* 366:557–559
- Zienkiewicz OC, Taylor R (1989) *The finite element method, basic formulation and linear problems*, vol 1. McGraw-Hill, London 648
- Zienkiewicz OC, Taylor R (1991) *The finite element method, solid and fluid mechanics dynamics and non-linearity*, vol 2. McGraw-Hill, London 807